Supporting Information

Reversible light-directed self-organized 3D liquid crystalline photonic nanostructures doped with azobenzene-functionalized bent-shaped molecules

Meng Wang,[a, b] *Wei Hu,*[c] *Ling Wang,*[d] *Duan-Yi Guo,*[e] *Tsung-Hsien Lin,*[e] *Lanying Zhang,*[b, f] *and Huai Yang**[b, f]

a. Department of Materials Science and Engineering, School of Mechanical Electronic and Information Engineering, China University of Mining and Technology-Beijing, Beijing 100083, P. R. China.

b. Department of Materials Science and Engineering, College of Engineering, Peking University, Beijing 100871, P. R. China.

c. Department of Chemistry and Chemical Engineering, School of Chemistry and Biological Engineering, University of Science and Technology Beijing, Beijing, 100083, P. R. China.

d. Artie McFerrin Department of Chemical Engineering, Texas A&M University, College Station, Texas 77843, United States.

e. Department of Photonics, National Sun Yat-sen University, Kaohsiung 80424, Taiwan.

f. Key Laboratory of Polymer Chemistry and Physics of Ministry of Education, Peking University, Beijing 100871, P. R. China.

* E-mail: yanghuai@pku.edu.cn.

1. Synthesis and characterization

1.1 General procedures for the synthesis of azobenzene-functionalized bent-shaped molecules

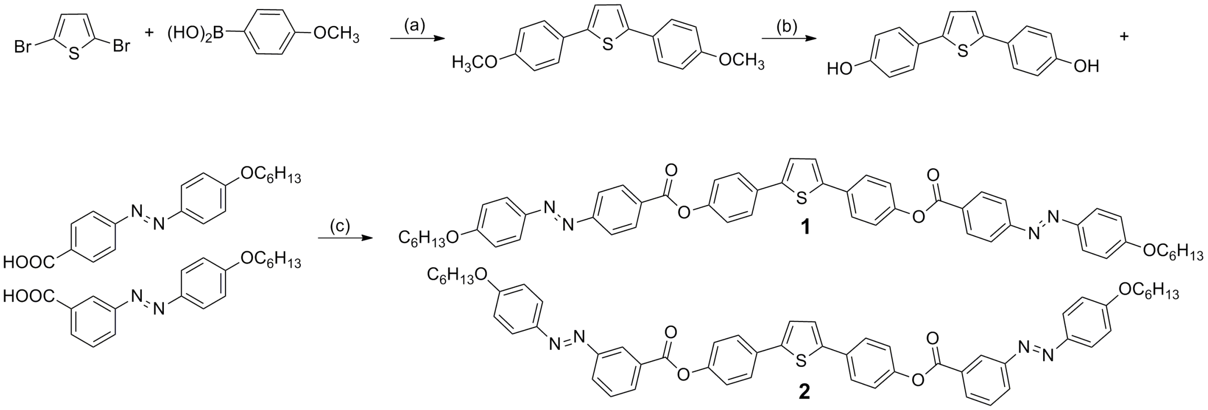

Scheme S1. Synthetic routes to the target compounds. Reagents and conditions: (a) $Pd(PPh_3)_4$, aq. K_2CO_3, alcohol, toluene, 70 ºC; (b) BBr_3, 0 ºC; (c) DCC, DMAP, CH_2Cl_2, RT.

All chemicals and solvents were purchased from commercial supplies and used without further purification. 2,5-dibromothiophene (9.67 g, 0.04 mol), tris(triphenylphosphine)palladium (0.5 g, 0.5 mol%) were dissolved in a mixture of alcohol (100 mL) and saturated sodium carbonate solution (0.33 mol) under argon. A solution of (4-methoxyphenyl)boronic acid (16.7 g, 0.11 mol) in toluene (50 mL) was added within 10min via a cannula. The solution was stirred at 70 ºC for 20 h. After agitation, the solution was quenched with pure water and the organic phase was dried over anhydrous magnesium sulfate ($MgSO_4$). Filtration through silica using dichloromethane/mineral ether and recrystallization from ethanol yielded pale yellow powders of 2,5-bis(4-methoxyphenyl)thiophene (4.7 g, 40%).

A 200 mL Schlenk flask was charged with 2,5-bis(4-methoxyphenyl)thiophene (4.7 g, 0.016mol) and dry dichloromethane (50 mL) under argon. In a separate flask, the boron tribromide (4.7 mL, 0.048 mol) was dissolved in dry dichloromethane (10 mL) and added to the reaction flask via a cannula at -78 ºC. The yellow solution was allowed to warm up to room temperature and was stirred at room temperature for 24 h. After that, the deionized water (50 mL) was added dropwise into the flask at -78 ºC, and the resulting mixture was stirred for 12 h at room temperature. After agitation, the reaction mixture was poured into 400 mL of deionized water and a dark green colored precipitate was filtered off. The crude product was then recrystallized from acetidin for three times to yield 2,5-bis(4-hydroxyphenyl)thiophene as green solid powders (3.7 g, 80%).

(E)-4-((4-(hexyloxy)phenyl)diazenyl)benzoic acid (0.65 g, 2 mmol), 2,5-bis(4-hydroxyphenyl)thiophene (0.27 g, 1 mmol) and N, N'-dicyclohexylcarbodiimide (DCC) (0.62 g, 3 mmol) in dichloromethane (50 mL) with catalytic amount of 4-dimethylamiopyridine (DMAP) (0.036 g, 0.3 mmol) were stirred at room temperature for 24 h. N, N'-dicyclohexylurea formed was filtered off. The filtrate was washed with deionized water and dried over $MgSO_4$. Solvent was removed under the reduced pressure and chromatographed over a column of silica gel using acetidin/ mineral ether as an eluent, and then recrystallized from acetidin yielded orange colored powders of 1 (0.4 g, 50 %). The compound 2 was synthesized under same procedure except using (E)-3-((4-(hexyloxy)phenyl)diazenyl)benzoic acid.

1.2 Characterization

H and ^{13}C NMR spectra were recorded by Varian 300 MHz and Bruker 500 MHz spectrometer using $CDCl_3$ as solvents. The mesophase behaviors and phase transition temperatures were confirmed by differential scanning calorimeter (PerkinElmer DSC8000) at a scanning rate of 10.0 ºC/min and polarized optical microscope (Carl Zeiss, AxioVision SE64) investigation. The UV-Vis absorption spectra of the two compounds in CH_2Cl_2 solvent at 25 ºC upon UV and visible light irradiation were detected by a UV/VIS/IR spectrophotometer (Perkin–Elmer Lambda 950) in transmission mode at normal incidence. The UV and visible light irradiation was carried out with the help of light sources with wavelength of 365 or 450 nm. A white light source and a fiber spectrometer (Avantes, AvaSpec-ULS2048) were used to collect the reflection spectra. Kossel diagrams were measured in the back focal plane of the objective in a Bertrand-lens-inserted microscope and a 440 nm light with a bandwidth of 10 nm was employed as the light source. Grandjean-Cano wedge cell (KCRK-07, tan θ = 0.0196, EHC) was used for the observation of disclination line to calculate the pitch.

Compound 1. ^{1}H NMR (500 MHz, $CDCl_3$) δ (ppm): 8.39 - 8.31 (m, 4H), 7.98 (m, 8H), 7.72 - 7.64 (m, 2H), 7.52 (t, *J* = 7.8 Hz, 2H), 7.36 - 7.30 (m, 2H), 7.28 (t, *J* = 7.8 Hz, 2H), 7.25 - 7.18 (m, 2H), 7.03 (d, *J* = 8.3 Hz, 4H), 4.07 (t, *J* = 6.6 Hz, 4H), 1.89 - 1.27 (m, 16H), 0.96 - 0.89 (m, 6H). ^{13}C NMR (100 MHz, $CDCl_3$) δ (ppm): 166.27, 162.09, 152.82, 146.75, 131.66, 130.98, 129.05, 126.20, 124.99, 124.04, 123.98, 114.78, 114.27, 68.44, 65.43, 31.58, 31.49, 29.16, 28.72, 25.72, 25.70, 22.60, 22.56, 14.02.

Compound 2. ^{1}H NMR (500 MHz, $CDCl_3$) δ (ppm): 8.52 (t, *J* = 1.7 Hz, 2H), 8.13 - 8.09 (m, 2H), 8.05 (m, 2H), 7.96 - 7.91 (m, 8H), 7.57 (t, *J* = 7.8 Hz, 2H), 7.05 - 6.98 (m, 8H), 6.95 - 6.86 (m, 1H), 6.76 - 6.70 (m, 1H), 4.36 (t, *J* = 6.7 Hz, 2H), 4.05 (t, *J* = 6.6 Hz, 2H), 1.87 - 1.30 (m, 16H), 0.95 - 0.88 (m, 6H). ^{13}C NMR (100 MHz, $CDCl_3$) δ (ppm): 166.27, 162.10, 152.81, 146.74, 131.66, 130.98, 129.05, 126.20, 125.01, 124.04, 114.79, 68.44, 65.43, 31.58, 31.49, 29.16, 28.72, 25.72, 25.70, 22.60, 22.56, 14.02.

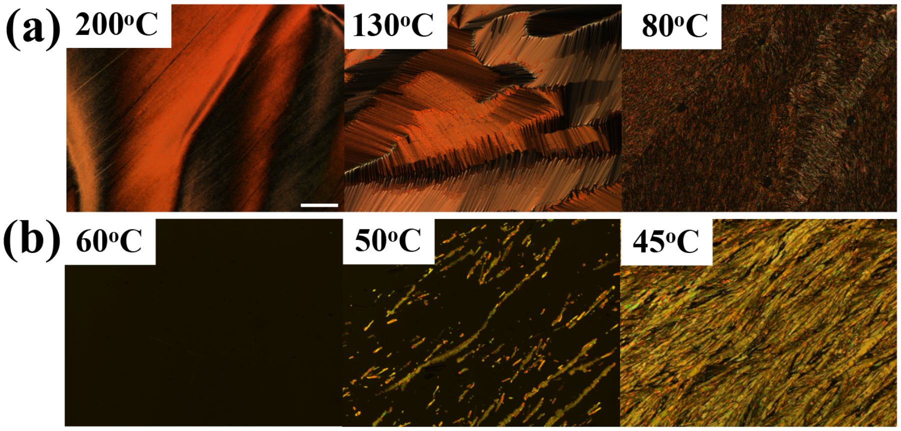

Figure S1. The POM textures of the two bent-shaped molecules of (a) compound 1 and (b) compound 2 at different temperature during cooling cycle.

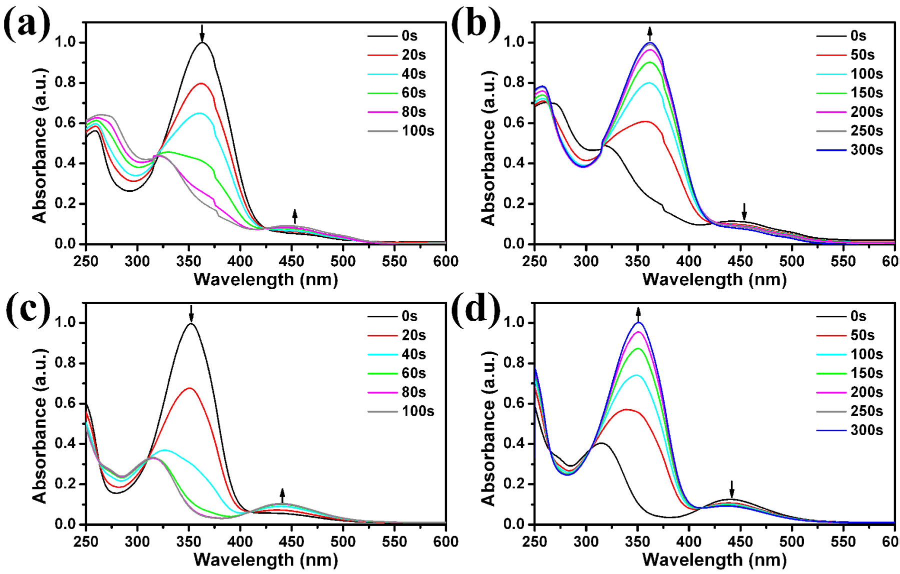

Figure S2. The UV-Vis absorption spectra of the two compounds in CH_2Cl_2 solvent at 25 °C upon UV and visible light irradiation. Absorption spectrum of (a) compound 1 and (c) compound 2 irradiated by UV light. The recovery spectrum of (b) compound 1 and (d) compound 2 irradiated by visible light.

For compound 1, the absorption peak at around 366 nm caused by the π-π* transition band of trans isomers decreased upon UV irradiation (365nm, 2.0 $mWcm^{-2}$), while the n-π* transition band of cis isomers at around 441 nm increased continually with irradiation time. The absorption peak changed little after irradiation for about 100 s, indicating that the photostationary state had been attained. Under visible light irradiation (450 nm, 5 mWcm^{-2}), the absorption bands returned to the initial states due to the rapidly reversible isomerization and the photostationary state was obtained within 300 s. Spectral bands and the isomerization properties of compound 2 were similar to 1 except for little shift in the absorption maxima.

2. Study of BP samples doped with azobenzene-functionalized bent-shaped molecules

2.1 Phase transition and BP temperature of the samples

Table 1. The liquid crystalline composites prepared, phase transition temperature during cooling from isotropic state and corresponding BP temperature range.

Sample	Composition/ wt%			Transition temperature/^{o}C				BP range /^{o}C
No.	SLC-4	R5011	R811	1	I - BP II	BP II - BP I	BP I - Ch	ΔT
0	90.0	2.6	7.4	0.0	63.5	61.0	57.0	6.5
A1	89.5	2.6	7.4	0.5	63.8	62.9	54.2	11.6
A2	89.0	2.6	7.4	1.0	65.2	-	50.6	14.6
A3	88.0	2.6	7.4	2.0	67.5	-	55.3	12.2
A4	87.0	2.6	7.4	3.0	68.7	-	58.4	10.3
A5	86.0	2.6	7.4	4.0	Phase separation			
	SLC-4	R5011		2	I - BP II	BP II - BP I	BP I - Ch	ΔT
B1	89.5	2.6	7.4	0.5	62.9	56.7	54.4	8.5
B2	89.0	2.6	7.4	1.0	62.5	54.3	52.7	9.8
B3	88.0	2.6	7.4	2.0	60.3	51.8	49.8	10.5
B4	87.0	2.6	7.4	3.0	58.0	49.2	47.6	10.4
B5	86.0	2.6	7.4	4.0	54.5	45.6	44.2	10.3
B6	80.0	2.6	7.4	10.0	41.0	35.9	34.6	6.4

ΔT is the temperature range of BPs between phase transition temperatures of I-BP II and BP I-Ch.

2.2 Phase transitions before or under UV irradiation

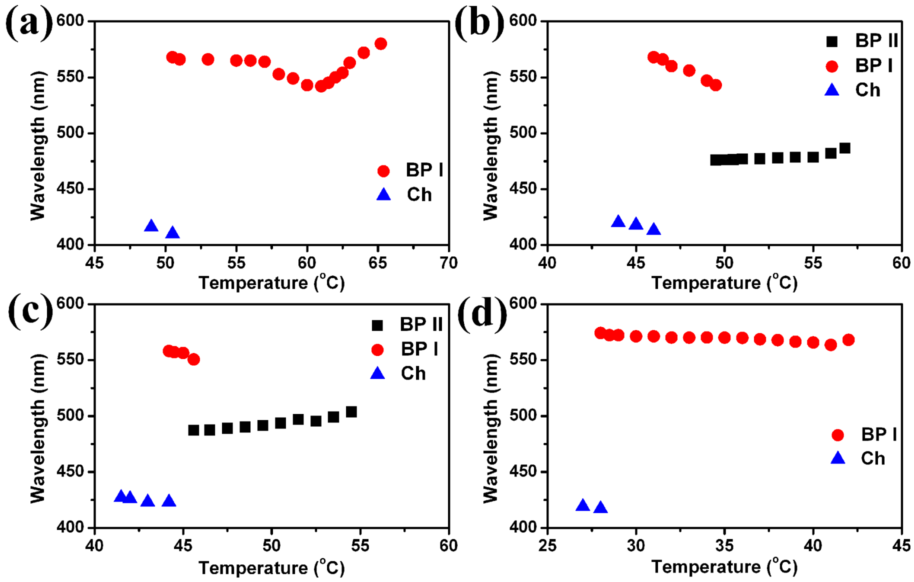

Figure S3. The peak wavelength of reflection band at different temperature during cooling cycle for (a) A2, (b) A2 under UV irradiation, (c) B5, and (d) B5 under UV irradiation.

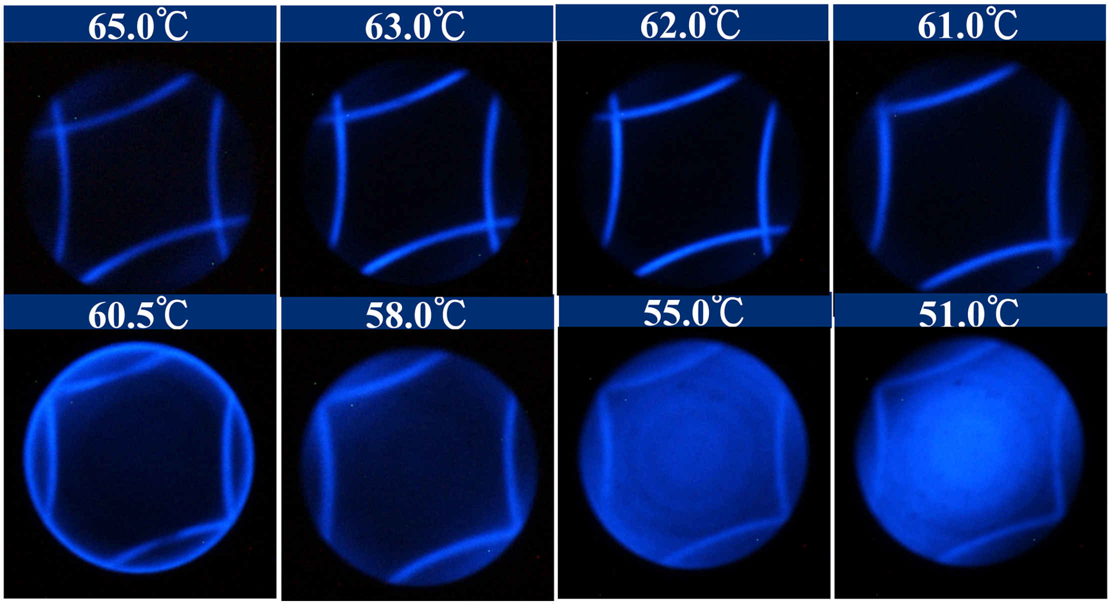

Figure S4. The Kossel diagram of sample A2 at different temperature during cooling cycle.

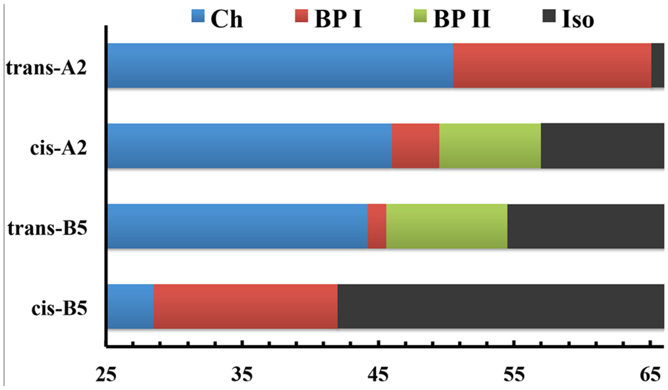

Figure S5. The phase transition temperature of sample A2 and sample B5 before (trans-) and under (cis-) UV light irradiation.

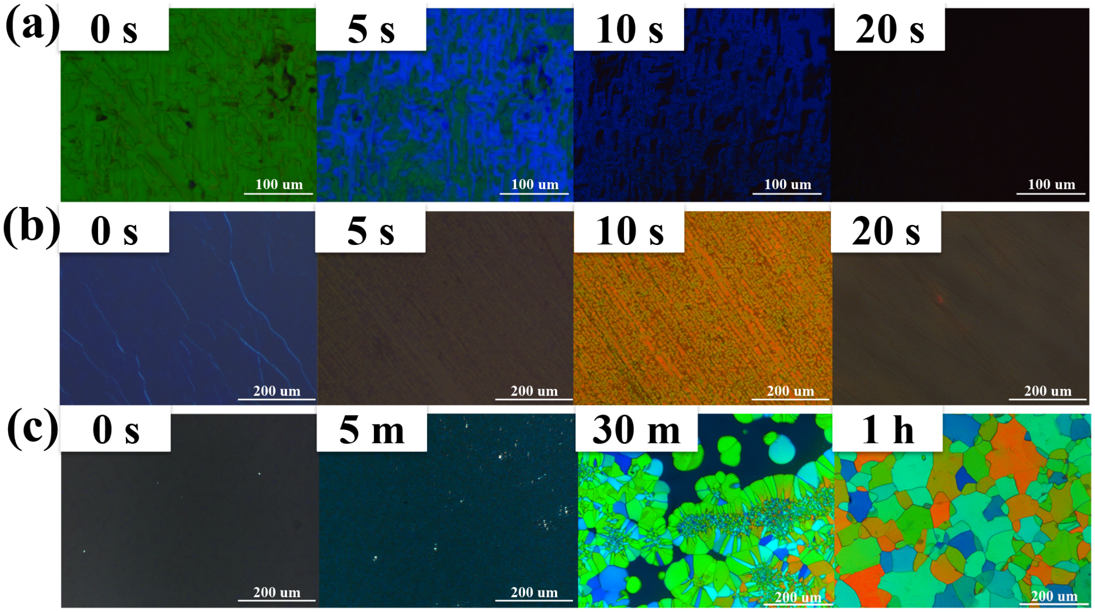

Figure S6. Temporal-dynamic POM textures under UV irradiation. (a) A2 irradiated at 55.0 ºC with UV intensity of 1.0 mW/cm^2. (b) B5 irradiated at 43.0 ºC with UV intensity of 5.0 mW/cm^2. (c) UV Irradiated B5 kept in dark for a certain time.

2.3 The influence of bent-shaped molecules to elastic constants of the host LC

The elastic constants of the pure SLC-4 (sample 0) and mixtures doped bent-shaped molecule 1 (smaple A) and 2 (sample B) in 1.0 wt% respectively were measured by the capacitance methods, and the results were shown in Table 2. In this concentration, the clearing points from N to I changed subtlety in both case.

Table 2. The parameters of the LC mixtures measured at different temperature.

Smaple NO.	Tmeperature/^{o}C	K_{11}	K_{22}	K_{33}	$\varepsilon_{//}$	$\varepsilon_{\perp}$	$\Delta\varepsilon$	K_{33}/K_{11}
0	20.0	10.0	5.0	14.2	55.8	8.1	47.7	1.4
0	30.0	8.2	4.1	10.7	49.0	7.7	41.2	1.3
0	40.0	7.1	3.5	8.0	41.8	7.6	34.2	1.1
0	50.0	6.2	3.1	5.5	35.3	7.3	27.9	0.9
0	60.0	5.3	2.7	4.2	30.0	7.3	22.8	0.8
A	20.0	10.2	5.1	15.0	54.3	7.7	46.7	1.5
A	30.0	8.6	4.3	12.2	46.9	7.6	39.3	1.4
A	40.0	7.4	3.7	9.4	40.3	7.5	32.8	1.3
A	50.0	6.6	3.3	6.5	34.7	7.3	27.4	1.0
A	60.0	5.6	2.8	4.9	29.7	7.2	22.5	0.9
B	20.0	9.0	4.5	12.9	49.0	7.7	41.3	1.4
B	30.0	7.4	3.7	9.4	42.2	7.6	34.5	1.3
B	40.0	6.3	3.2	6.3	36.0	7.3	28.6	1.0
B	50.0	5.4	2.7	4.5	30.7	7.3	23.4	0.8
B	60.0	4.4	2.2	3.4	26.0	7.5	18.5	0.8

2.4 The influence of photoisomerization to chirality

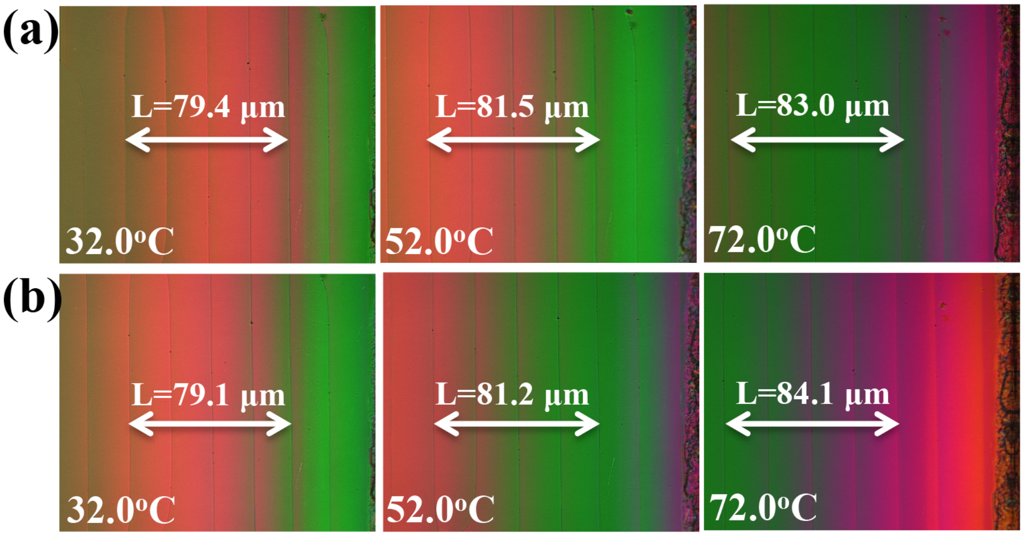

Figure S7. The POM textures at different temperature of a sample composited by SLC-4/R5011/1 (98.4%/0.6%/1.0% in weight). (a) Without UV irradiation and (b) under UV irradiation.

2.5 The speculation of photo-responsive behavior

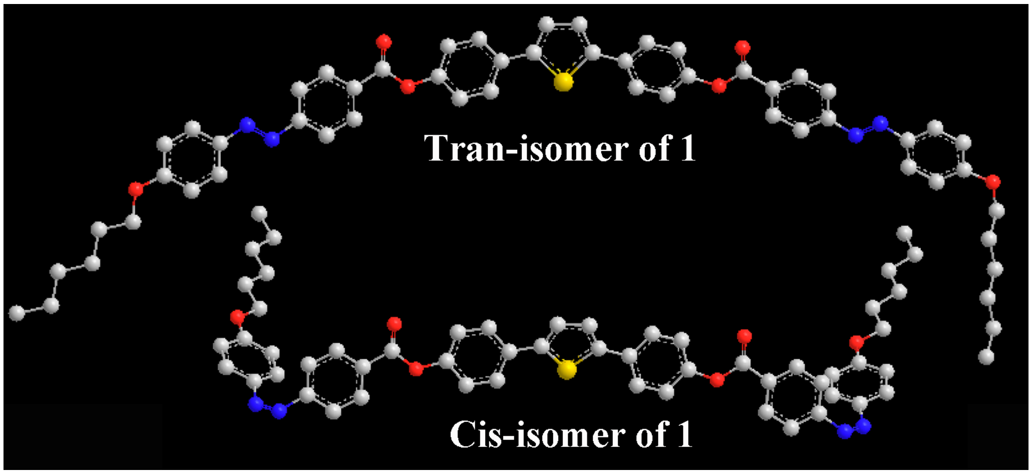

Figure S8. The optimized structures of trans and cis-form of compound 1 obtained by Gaussian 03 calculations at B3LYP/6-31G level.